AD-A139 233 NEUTRAL GAS PLASMA INTERACTIONS AND CRITICAL IONIZATION 1/1
VELOCITY PHENOMEN..(U) MARYLAND UNIV COLLEGE PARK DEPT
OF PHYSICS AND ASTRONOMY K PAPADOPOULOS 11 NOV 83
UNCLASSIFIED AP-83-083 N00014-79-C-0665 F/G 20/9 NL

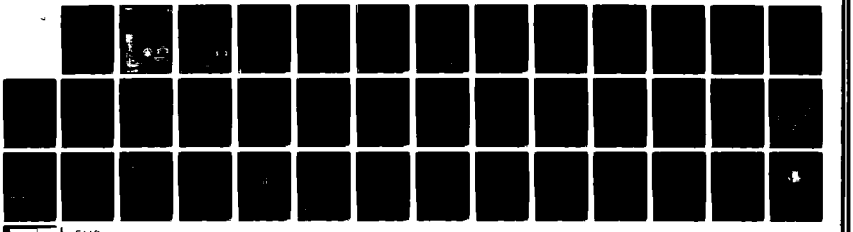

END
DATE FILMED
5-84
DTIC

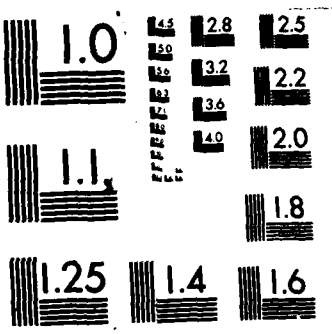

# NEUTRAL GAS PLASMA INTERACTIONS
# AND
# CRITICAL IONIZATION VELOCITY PHENOMENA

by

K. Papadopoulos




UNIVERSITY OF MARYLAND
DEPARTMENT OF PHYSICS AND ASTRONOMY
COLLEGE PARK, MARYLAND

# NEUTRAL GAS PLASMA INTERACTIONS
# AND
# CRITICAL IONIZATION VELOCITY PHENOMENA

by

K. Papadopoulos

SECURITY CLASSIFICATION OF THIS PAGE (When Data Entered)

## REPORT DOCUMENTATION PAGE

READ INSTRUCTIONS BEFORE COMPLETING FORM

| | |
|---|---|
| 1. REPORT NUMBER<br>University of Maryland<br>Report AP 83-083 | 2. GOVT ACCESSION NO.<br>AD-A139 233 |
| 3. RECIPIENT'S CATALOG NUMBER | |
| 4. TITLE (and Subtitle)<br>Neutral Gas Plasma Interactions and Critical Ionization Velocity Phenomena | 5. TYPE OF REPORT & PERIOD COVERED<br>Interim report on a continuing problem |
| | 6. PERFORMING ORG. REPORT NUMBER |
| 7. AUTHOR(s)<br>K. Papadopoulos | 8. CONTRACT OR GRANT NUMBER(s)<br>N00014-79C-0665 |
| 9. PERFORMING ORGANIZATION NAME AND ADDRESS<br>University of Maryland<br>Department of Physics and Astronomy<br>College Park, MD 20742 | 10. PROGRAM ELEMENT, PROJECT, TASK AREA & WORK UNIT NUMBERS |
| 11. CONTROLLING OFFICE NAME AND ADDRESS<br>Office of Naval Research<br>Arlington, VA 22217<br>NASA<br>Washington, DC | 12. REPORT DATE<br>13. NUMBER OF PAGES<br>37 |
| 14. MONITORING AGENCY NAME & ADDRESS(if different from Controlling Office) | 15. SECURITY CLASS. (of this report)<br>UNCLASSIFIED<br>15a. DECLASSIFICATION/DOWNGRADING SCHEDULE |

16. DISTRIBUTION STATEMENT (of this Report)

Approved for public release; distribution unlimited.

17. DISTRIBUTION STATEMENT (of the abstract entered in Block 20, if different from Report)

18. SUPPLEMENTARY NOTES

Text of an invited talk (6A3) presented at the Twenty-fifth Annual Meeting of the Division of Plasma Physics, Los Angeles, CA; 7-11 November 1983.

19. KEY WORDS (Continue on reverse side if necessary and identify by block number)

Critical ionization velocity, Neutral gas plasma interaction,

Lower hybrid waves, Space Shuttle Glow, Comets

20. ABSTRACT (Continue on reverse side if necessary and identify by block number)

The interplay of collisional and collisionless phenomena in the interaction of a magnetoplasma streaming through neutral gas produces some of the most fascinating plasma physics phenomena. A key notion controlling such interactions is the existence of a "critical velocity" ($U_c$) effect postulated in an ad hoc fashion by Alfven, in his model of the formation of the solar system. According to Alfven's postulate, whenever the relative velocity between a neutral gas and a streaming magnetoplasma exceeds a value $U_c \equiv \sqrt{2E_i/M}$, where $E_i$ is the

DD FORM 1 JAN 73 1473 EDITION OF 1 NOV 65 IS OBSOLETE

S/N 0102-LF-014-6601

SECURITY CLASSIFICATION OF THIS PAGE (When Data Entered)

ABSTRACT (continued)

ionization energy and M the mass of the neutral atoms, rapid ionization and anomalous momentum coupling occurs. Guided by recent laboratory and space experiments and plasma physics underlying the interaction. This is followed by a discussion of its relevance to the formation of the solar system and cometary tails, its controlling effect on plasma centrifuges and homopolar generators, and the fascinating possibility that critical velocity phenomena are controlling the space shuttle environment, transforming it into an artificial comet.

AP 83
083

# Neutral Gas Plasma Interactions

# and

# Critical Ionization Velocity Phenomena*

by

K. Papadopoulos
University of Maryland
Department of Physics and Astronomy

*Text of an invited talk (6A3) presented at the Twenty-fifth Annual Meeting of the Division of Plasma Physics, Los Angeles, CA; 7-11 November 1983.

## Abstract

The interplay of collisional and collisionless phenomena in the interaction of a magnetoplasma streaming through neutral gas produces some of the most fascinating plasma physics phenomena. A key notion controlling such interactions is the existence of a "critical velocity" ($U_c$) effect postulated in an ad hoc fashion by Alfven, in his model of the formation of the solar system. According to Alfven's postulate, whenever the relative velocity between a neutral gas and a streaming magnetoplasma exceeds a value $U_c \equiv \sqrt{2E_i/M}$, where $E_i$ is the ionization energy and M the mass of the neutral atoms, rapid ionization and anomalous momentum coupling occurs. Guided by recent laboratory and space experiments and plasma physics theory we present the basic plasma physics underlying the interaction. This is followed by a discussion of its relevance to the formation of the solar system and cometary tails, its controlling effect on plasma centrifuges and homopolar generators, and the fascinating possibility that critical velocity phenomena are controlling the space shuttle environment, transforming it into an artificial comet.


Square root of (2 E sub i/M),

## 1. A Historical Prospective:

The critical ionization velocity (CIV) concept was introduced by Aflven in a highly inspired fashion as a hypothesis. The CIV hypothesis stated that, if the the streaming velocity U between a neutral gas and a magnetized plasma exceeds a critical value $U_c$ defined as $U_c \equiv [\frac{2E_i}{M}]^{1/2}$, i.e.

$$U \geq U_c \qquad (1)$$

where $E_i$ is the ionization energy and M the mass of neutrals, we have the following phenomena:

(i) Abrupt increase in ionization

(ii) Strong momentum coupling between the gas and the plasma

(iii) The velocity U quickly approaches $U_c$

The idea was based on a simple energy balance. Namely, a neutral atom ionized and stopped by the plasma releases enough energy to ionize another atom. The condition $U \geq U_c$ for CIV phenomena is equivalent to the energy balance argument, $\frac{1}{2} MU^2 \geq E_i$, mentioned above. The CIV hypothesis was the cornerstone of Alfven's theory[2] for the formation of secondary bodies around a central body in solar systems. This theory, known as hetegonic theory from the Greek (companion) and (formation), deals with the formation of the planets (i.e. companion bodies) around the Sun, satellite systems around magnetized planets (i.e. Jupiter and its satellites, Saturn and its satellites) e.t.c.. By noting that the most abundant elements in the solar system fall in three bands of critical ionization velocities (Fig. 1), one for $U_{c1} \approx 5\text{-}7 \frac{km}{sec}$, one for $U_{c2} \approx 13\text{-}16 \frac{km}{sec}$ and one for $U_{c3} \approx 35\text{-}40 \frac{km}{sec}$, Alfven[2,3] predicted that there will be three discrete bands of satellites as a function of distance from the central body. To reach this

conclusion he postulated the following sequence of events. A neutral cloud falling towards a central body accelerates due to the gravity (Fig. 2). When its velocity reaches $U_{c1}$, which corresponds to a radius $R_1$ away from the central body given by the relationship $\frac{GM_cM}{R_1} = \frac{MU_{c1}^2}{2}$, where G and $M_c$ are the gravitational constant and mass of the central body, the CIV phenomenon occurs and a fraction of the neutral gas is ionized and trapped by the magnetic field in a zone about $R_1$. The plasma emplaced in that region subsequently accretes forming the secondary bodies (i.e. planets or satellites). The non-ionized part of the gas continues falling till a radius $R_2 < R_1$ where $\frac{GM_c}{R_2} = \frac{1}{2} U_{c2}^2$ at which point plasma emplacement and subsequent accretion form a second band of secondary bodies. In a similar fashion a third band of secondary bodies forms at a distance $R_3$. The relationship between the radius $R_j$, j = 1-3, and $U_{cj}$ becomes clearer by using the specific gravitational potential $\Gamma_j \equiv \frac{M_c}{R_j}$. We then have the relationship

$$2G\Gamma_j = U_{cj}^2 \qquad (2)$$

To demonstrate such a relationship for solar system Alfven[1-3] presented in addition to Fig. 1, the diagram of Fig. 3 which, "with some imagination", can be construed as consistent with his hypothesis.

The CIV suggestion caused an immediate and rather justified controversy given its empirical and intuitive approach as well as the many puzzles raised in view of the rather uniform element abundance in the secondary bodies. The process was even thought to be energetically impossible since the available free energy for ionization is the energy at the center of mass system. The conventional wisdom at the time dictated that ion-neutral collisions was the

only means of energy and momentum transfer; therefore the available free energy E of the system was bounded by

$$E = \frac{1}{2}\left(\frac{M_n M}{M_n + M}\right) U^2 \leq \frac{1}{2} M_n U^2 \qquad (3)$$

where $M_n$ is the mass of the neutrals.

## 2. Laboratory Search for CIV:

Unexpected support for the CIV hypothesis came in the early sixties[4-8] from experiments on rotating plasmas whose archetype model is the homopolar generator (Fig. 4). Fast $\frac{\underline{E}\times\underline{B}}{B^2}$ rotation was required for three diverse purposes. Energy storage[4-6] plasma confinement[7] and chemical element and isotope separation[8]. All these experiments were plagued by limitations on the discharge voltage, which controlled the rotation speed. It was found that over two orders of magnitude in discharge current and three in neutral pressure the discharge voltage was clamped so that the value of the drift $\frac{E}{B} = U_c$. This is shown graphically in Fig. 5. These results prompted a series of experiments with coaxial guns[9-11] in the 1970's. The results demonstrated rather conclusively the CIV hypothesis and gave us a variety a clues concerning the physical processes involved. Fig. 6a shows the coaxial gun configuration and the experimental results of Danielson[9] which are rather typical of this set of experiments. It is worth noting that the measurements indicated

(i) The presence of energetic (80-100 eV) electrons

(ii) Electrostatic turbulence in the lower hybrid ($\omega_{LH}$) range

(iii) Momentum coupling length $L \ll r_i$ where $r_i$ the ion gyroradius, with $L \sim \frac{1}{B}$ (Fig. 6b) scaling.

3. Physical Foundations of CIV:

The above experimental results coupled with major advances in our understanding of the non-linear plasma processes in the lower hybrid range[11-14] brought us to a new plateau in understanding the physics of CIV. The presence of energetic electrons led to the resolution of the free energy puzzle above. The energy transfer goes from the newly born ions to electrons so that the center of mass energy is basically equal to the laboratory energy. The collisionless scale for energy transfer $L < r_i$ and the presence of lower hybrid turbulence led to the search for collective plasma processes with scale lengths shorter than $r_i$ (i.e. unmagnetized ions) and frequency $\omega_{LH}$. The following physical picture has emerged[15-19]. Consider a neutral gas flowing across a magnetized plasma with velocity U. Associated with it is a small fraction of ionization constituting a small ion beam of density $n_s$ streaming through the magnetized plasma (Fig. 7). The small fractional ionization can be due to charge exchange, photoinization or impact ionization. Its level is of no importance and is similar to the assumption of a free electron in avalanche ionization, or of background noise in plasma instability calculations. If a collisionless plasma instability can transfer energy from the ion beam (i.e. free-energy $\frac{1}{2} n_s MU^2$) to electrons with energy above $E_i$ on a time scale faster than ionization, a discharge (i.e. avalanche ionization) becomes possible. An energy flow diagram appears in Fig. 8. $\eta_1$ is the efficiency of energy transfer from the ion beam to electrons; $\eta_2$ is the fraction of energy transferred to hot electrons (by "hot electrons" we define here electrons with energy above $E_i$); $\eta_3$ is the fraction of the hot electrons that make ionizing collisions before they leave the system. Evaluation of $\eta_1$, $\eta_2$, $\eta_3$ is a plasma physics problem and their determination depends on the particular system under consideration. We will discuss a

specific example in the next section. On the basis of Fig. 8 and with the definitions of $\eta_1$, $\eta_2$, $\eta_3$ given above we can use energy arguments to refine Alfven's CIV criterion. The rate of free energy available for collisionless energy transfer is given by

$$F_1 = \left(\frac{dn_s}{dt}\right) \frac{1}{2} MU^2 \tag{4}$$

where $\left(\frac{dn_s}{dt}\right)$ is the ionization rate. The rate of free energy available for ionization is

$$F_2 = \eta_1\eta_2\eta_3 F_i \tag{5}$$

The rate at which energy is consumed in ionization is

$$F_3 = \left(\frac{dn_s}{dt}\right) E_i \tag{6}$$

A discharge is energetically possible only if

$$F_2 > F_3 \tag{7}$$

From (4)-(7) it is easy to derive the energetically necessary condition for CIV as

$$U > \frac{1}{[\eta_1\eta_2\eta_3]^{1/2}} U_c \tag{8}$$

We recover condition (1) if $\eta_1 = \eta_2 = \eta_3 = 1$, i.e. all the free energy goes to electrons with energy above $E_i$ that stay long enough in the system to produce ionizing collisions.

4. The Plasma Physics of CIV:

Taking advantage of the fact that for most systems of interest the plasma time scales (which in our case turn out to be of the order $\omega_{LH}^{-1}$) are much shorter than ionization time scales, we can use a multiple time scale approach to the problem, freezing the ionization time scale and addressing the energy transfer problem from the newly born ions to ionizing electrons as a non-linear plasma problem under homogeneous space time plasma conditions. The velocity distribution of the system is shown in Fig. 7, and the key plasma physics question is the determination of $\eta_1$, $\eta_2$, $\eta_3$. $\eta_3$ depends critically on the finite system size, formation of sheaths e.t.c. A generic form of $\eta_3$ is

$$\eta_3 = 1 - \exp(-\nu_i \tau_c) \tag{9}$$

where $\nu_i$ is the rate of ionization and $\tau_c$ the confinement time of the "hot" electrons. For $\nu_i \tau_c \gg 1$, which is a modified form of the Townsend condition, $\eta_3 = 1$. This is the case we will address here. Notice that our treatment is easily generalized to the case where $\nu_i \tau_c \gtrsim 1$, since in this case

$$\eta_3 = \nu_i \tau_c \tag{10}$$

The values of $\eta_1$ and $\eta_2$ are also a function of the collisionality and the other parameters of the system and should be determined on a case by case basis. As a generic example of the type of considerations that should be followed we will use the analogy of the collective interactions expected for the configuration of Fig. 7 with the classical electron beam plasma instability theory[20] to determine $\eta_1$ and $\eta_2$. For the electrostatic case, which implies $U < v_A$ where $v_A$ the Alfven speed, the dispersion relation is

$$\frac{\alpha\,\omega_i^2}{(\omega-\underline{k}\cdot\underline{U})^2} + \frac{\omega_e(\frac{k_z}{k})^2}{\omega^2} + \frac{\omega_i^2}{\omega^2} = 1 + \frac{\omega_e^2}{\Omega_e^2} \qquad (11a)$$

where $\alpha = \frac{n_s}{n_o}$. Eq. (11a) has been derived for $r_e < \frac{1}{k} < r_i$, $\Omega_i < \omega < \Omega_e$ and cold electrons and ions[11-14]. Eq. (11a) can be written as

$$\frac{\alpha\,\omega_{LH}^2}{(\omega-\underline{k}\cdot\underline{U})^2} + \frac{\omega_{LH}(1+\frac{M}{m}\frac{k_z^2}{k^2})}{\omega^2} = 1 \qquad (11b)$$

which demonstrates the analogy with the standard electron-electron two stream instability. The non-linear saturation of electron beam plasma instabilities in the absence of strong turbulence effects[21], has been discussed on the basis of quasilinear theory[20] or cold coherent beam plasma theory[22]. We follow here the quasilinear analysis as presented in ref. 15-18. Notice, that the more exact analysis along the negative energy wave cold beam plasma theory is more complex[23] and produces small variation over the quasilinear result. It was noted by Formisano et al.[15] and Galeev[16], that if the instability stabilizes by forming a plateau (Fig. 9a) $\frac{1}{3}$ of its energy stays in the ions, while $\frac{2}{3}$ is available for electron heating so that $\eta_1 = \frac{2}{3}$. Papadopoulos[17],19 carried a quasilinear analysis of the electron energy transfer. It was found that electron tails are formed in the direction parallel to the magnetic field

(Fig. 9b) with a lower energy given by $\frac{1}{2} MU^2$ and an upper energy $6\,\frac{1}{2} MU^2$. The electron energy perpendicular to the field is an adiabatic invariant. Therefore

$$\eta_3 = \frac{\int_{U_c}^{\sqrt{3}U} dv\ v^2 f_T(v)}{\int_{U}^{\sqrt{3}U} dv\ v^2 f_T(v)} \tag{12a}$$

Taking $f_T(v)$ as a plateau we find that

$$\eta_3 = 1 - \frac{1}{3^{3/2}} \left(\frac{U_c}{U}\right)^3 \tag{12b}$$

From eqs. (8) and (12b), with $\eta_1 = 1$ and $\eta_2 = \frac{2}{3}$, we can easily recover the result of refs. 21, 22, i.e.

$$U > \left(\frac{2}{3}\right)^{1/2} U_c \tag{13}$$

as the CIV condition. A more detailled theory including slowing down due to momentum coupling as well as the role of collisionality and beam temperature on the collisionless transfer will appear elsewhere[23].

While this physical picture can account for bulk coupling in gas plasma interactions and for the coaxial gun experiments, a variation seems more appropriate for ionizing fronts[24] such as the ones formed in rotating plasmas. For plasma density gradient $L_N$ in the front with $L_N < r_i$, an electron drift develops such as shown in Fig. 10a. This can drive either the modified two stream or the lower hybrid drift instability, resulting in generation of hot electrons. The flow diagram of the process is shown in Fig. 10b, and results in a criterion of the type given by (13). A detailled analysis of this case is in progress.

From the above considerations the signatures of CIV are:

(i) Energetic electron tails and hot ions

(ii) Electrostatic waves in the lower hybrid range

(iii) Light emission.

In addition to these we expect that the presence of energetic electrons will produce electrostatic wave signatures near the plasma and upper hybrid frequency, and electromagnetic whistler waves. The latter waves will be produced by the energetic electrons which isotropize by emitting whistlers.

5. CIV in Space:

Evidence of CIV occurring in space is quite indirect due to the absence of experiments with in situ measurements. We briefly comment below on two situations. The first is an active ionospheric experiment discussed by Haerendel[25]. An explosive Ba release from a rocket generated a gas jet with velocity 6-10 $\frac{km}{sec}$ in the ionosphere ($U_c$ for Ba is 5 $\frac{km}{sec}$). The altitude of the gas injection was well in the earth's UV shadow, about 100 km below the UV terminator. For optical diagnostics sunlight is needed, but should be suppressed as a competing process to CIV. Thus the shaped charge was ignited in the earth's shadow and observed at the terminator which was illuminated. Any ionization produced at this time would appear in a sunlight as a field aligned streak of $Ba^+$, which after correction for the plasma drift, passes through the explosion point. The results indicated that over 30% of the $Ba^+$ cloud was ionized very near the injection point, before photonization becomes effective and with an upper limit of 1% on the thermal ionization due to the explosion (Fig. 11). The value of 30% was consistent with the fraction of Ba neutrals expected to have velocity perpendicular to the magnetic field above

$U_c$. CIV was invoked as the most probable cause for the anomalous ionization.

The second situation comes from cometary physics. When a comet enters the solar system sunlight generates a neutral gas environment around the cometary nucleus. The solar wind streaming across the comet generates the classic neutral gas streaming plasma situation expected for CIV phenomena. In fact an anomalous ionization process is required to account for the observed formation of the cometary tails and the subsequent momentum coupling to the solar wind, and even the formation of cometary bow shocks.

Unexpected evidence for CIV came from the recent flights of the space shuttle in a fashion that has raised the fascinating possibility that the space shuttle itself is an artificial comet. We discuss this next.

## 6. Is the Space Shuttle an Artificial Comet?

The possibility that the space shuttle can produce phenomena similar to the ones expected in CIV and the interaction of comets with the solar wind, is due to the following observation. When the tail of the space shuttle is ramming across the ionosphere the neutral density is seen to increase by $10^2$-$10^3$ times over the ambient. The cause is a combination of stagnation point effects, outgassing and surface gas emissions. Therefore, the space shuttle surrounded by its own atmosphere is moving across the ionospheric plasma at the orbital velocity ($\sim 8 \frac{km}{sec}$). The plasma environment around the sh[illegible]as measured by many instruments[26-30]. A summary of the observations i[illegible]5)

The plasma density (n) in the vicinity of the orbiter was often found several times and up to an order or magnitude higher than

the ambient plasma density ($n_o$). It is like an ionized cloud surrounding selective areas of spacecraft;

(ii) Energetic (10-100 eV) electron fluxes up to $10^{14}$el/cm$^2$sec were measured, with the maximum occurring during daytime conditions;

(iii) Ion fluxes with energies of up to 30 eV were observed, sometimes coincident with single or counter-streaming ion beams with 10 eV mean energy;

(iv) In addition to $O^+$, $NO^+$ and $O_2^+$, $H_2O^+$ which is not an ionospheric specie was observed, being on occasion the dominant species;

(v) An intense electrostatic broadband noise between low and high frequency cutoffs at 30 Hz and 20 kHz (i.e. around the lower hybrid frequency with shuttle motion Doppler shift) was observed, as well as plasma and whistler waves;

(vi) A gas layer of up to $10^{-5}$ torr was associated with surfaces ramming into atmospheric gases. Large pressure increases were observed during thruster operations and with payload bay doors closed;

(vii) Most of the plasma phenomena were intensified during daytime conditions and during thruster operations.

Associated with these plasma phenomena was an intense glow[31,32] on the surface. While the source of the glow and its potential analogy to the cometary glow is fascinating, it could also impose a major constraint in the utility of optical and infrared telescopes from the shuttle and other orbiting platforms. The similarity of the above signatures with the signatures expected from CIV theory and experiments lead Papadopoulos[17,19] to consider the shuttle as providing a rather definitive observation of CIV in space. We should, however, note that there is a difficulty with this interpretation.

The $U_c$ for O, $N_2$ and $CO_2$ is 12.8, 9.3 and 9.0 $\frac{km}{sec}$, while the shuttle moves with 8 $\frac{km}{sec}$. The resolution to this problem[19] is that the discharge is not self sustained without additional free energy sources. In ref. 17,19 such sources were identified as charge exchange and plasma reflection from the shuttle tail. Modest values of these effects allow the discharge around the shuttle to be maintained in a wet woodburner fashion. A detailled study of the fascinating possibility that the space shuttle behaves as a comet is presently under study.

## 7. Summary and Conclusions:

I have presented a summary of the modern understanding of CIV phenomena in the interaction of a magnetoplasma streaming through a neutral gas. It is obvious that while experimental and theoretical understanding has reached a new plateau many issues remain to be resolved. Some key problems are related to the CIV in multispecie situations, the spatial development of the neutral gas plasma interactions and the role of inhomogeneities, low density neutral gas situations where $\nu_i < \Omega_i$, high speed flows with $u > v_A$ etc. The universal role of the neutral gas plasma interactions in both laboratory and cosmical plasma warrants a higher level of attention than it has been given today. While the interdisciplinary character of the problem has probably discouraged the involvement of younger researchers, the richness of phenomena involved in the interplay of collisional and collisionless interactions presents many intellectual challenges and most probably a wealth of fascinating physical phenomena and potential applications in the coming years.

Acknowledgements:

I would first like to express my gratitude to G. Hearendel, who with his usual visionary attitude led my attention to the fascinating physics of CIV. Discussions with Dr. A. Drobbot, I. Kofsky, E. Möbius and R. Smith are greatfully acknowledged. The development of many of the ideas presented was generously supported by Science Applications International.

## References


1. H. Alfvén "On the Origin of Solar System" Oxford Univ. Press, 1954.
2. H. Alfvén and G. Arrhenius "Structure and Evolutionary History of the Solar System" D. Reidel Co., 1975.
3. H. Alfvén and C. Falthammar Cosmical Electrodynamics Oxford, at the Clarendon Press, 1963.
4. B. Angerth, L. Block, U. Fahleson and K. Soop Nucl. Fusion Suppl. Pt, 39, 1962.
5. B. Lehnert, J. Berstrøm and S. Holmberg Nucl. Fusion, 6, 231, 1966.
6. E. Møbius, A. Piel and G. Kimmel Z. Naturforsdhung, 34a, 405, 1979.
7. K. Boyer, J.E. Hammel, C.L. Longmire, D. Nagle, F. Ribe and W.B. Riesenfeld Proc. Conf. Geneva, 31, 319, 1958.
8. M. Krishnan and J.L. Hirschfield Phys. Rev. Lett., 46, 36, 1981.
9. L. Danielson Phys. Fl., 13, 2288, 1970.
   L. Danielson and N. Brenning Phys. Fl., 18, 661, 1975.
10. N. Brenning Plasma Phys., 23, 967, 1981.
11. M.A. Raadu J. Phys. D: Appl. Phys., 11, 363, 1978.
12. J. McBride, E. Oh, J. Boris and J. Orens Phys. Fl., 15, 2367, 1972.
13. M. Lampe and K. Papadopoulos Astrophys. J., 212, 886, 1977.
14. M. Tanaka and K. Papadopoulos Phys. Fl., 26, 1697, 1983.
15. D.V. Formisano, A.Galeev and R. Sagdeev Planet. and Space Sci., 30, 491, 1982.
16. A. Galeev and R. Sagdeev Sov. Phys., Plasma Physics (in press).
17. K. Papadopoulos Proceedings of Symposium on Active Experiments in Space ESA SP-165, p. 227, 2983.
18. E. Mobius ibid, p. 215, 1983.

19. K. Papadopoulos Radio Science (in press).

20. A. Vedenov and D. Ryutov Reviews of Plasma Physics Vol. 6, E. Leontovich (Editor) p. 1, 1972.

21. K. Papadopoulos Phys. Fl., 18, 1769, 1975.

22. W.E. Drummond, J.H. Malmberg, T.M. O'Neil, and J.R. Thompson Phys. Fl., 13, 2422, 1970.

23. K. Papadopoulos (in preparation).

24. E. Möbius, A. Piel and G. Himmel Z. Naturforsh. 34a, 405, 1979.

25. G. Haerendel Z. Naturforsh. 370, 728, 1983.

26. S. Shawhan and G. Murphy J. Spacecraft and Rockets (communicated).

27. J.M. Grebowsky, M.W. Paro, III, H.A. Taylor, Jr. and I.J. Eberstein AIAA Shuttle Environment and Operations, paper 83-2597, p. 47, 1983.

28. W. McMahon, R. Salter, R. Hills and D. Delorey ibid, paper 83-2598, p. 52, 1983.

29. G. Murphy, S. Shawhan and J. Pickett idbi paper 83-2599, 1983.

30 J. Rait Radio Science (in press).

31. S.B. Mende, O.K. Garriot and P.M. Banks Geophys. Res. Lett. 10, 122, 1983.

32. I. Kofsky and J. Barrett Radio Science (in press).

## Figure Captions

Figure 1 Critical ionization velocity and ionization potential of the most abundant elements. The left hand ordinate shows values of the gravitational potential energy and the right values of $U_c$. (ref. 2)

Figure 2 Schematic of plasma emplacement from a neutral cloud falling towards a magnetized central body.

Figure 3 Gravitational potential energy as a function of the mass of the central body for the planetary and satellite systems (ref. 2).

Figure 4 Rotating plasma in a homopolar configuration. (ref. 4)

Figure 5 Evidence for CIV in homopolar configurations (ref. 4)

(a) Voltage limitation as a function of B for various neutral pressures, showing $\frac{1}{B}$ dependence.

(b) Limiting voltage $V_L$ vs B for various species (O,D,H).

(c) $U_c$ vs applied current for seven gases.

Figure 6 (a) Coaxial gun configuration.

(b) Momentum coupling length for $H_e$ in Danielson's experiment (ref. 9). The front of the cloud was located at z = -5 cm.

(c) Initial vs final velocity for Hydrogen (ref. 9).

Figure 7 Neutral gas streaming through plasma and cross-field seed ion beam plasma velocity configuration.

Figure 8 Energy flow feedback for CIV.

Figure 9 (a) Seed ion beam quasilinear relaxation via plateau formation.

(b) Quasilinear electron tail formation parallel to B.

Figure 10 (a) Cross-field electron current generation for an ionizing front[24].

(b) Feedback diagram for ionizing fronts[24].

Figure 11 Situation of Hearendel's[25] Ba jet experiment. The CIV ionization, is termed as initial ionization, moved along B and was secmg at the terminator.

Figure 12 (a) Typical ambient ionospheric electrons fluxes[28].

(b) Enhanced electron fluxes around the shuttle.

Figure 13 Spectrum of lower hybrid waves near the shuttle[26].

Figure 14 Enhancement of electrostatic (kHz) waves during thruster operation[29].

Figure 15 Shuttle glow in the spacecraft tail under RAM conditions[31].

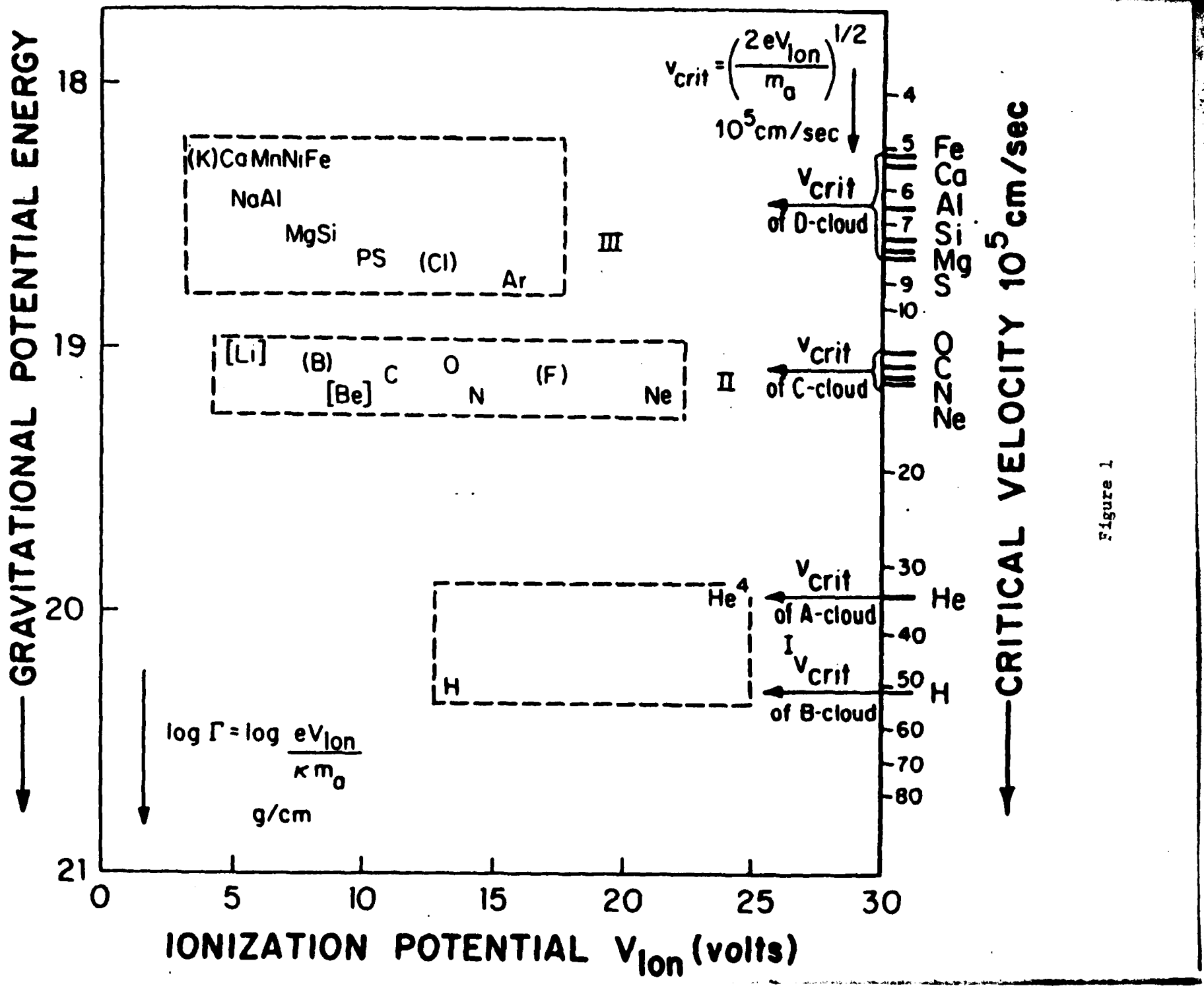
GRAVITATIONAL POTENTIAL ENERGY
CRITICAL VELOCITY $10^5$cm/sec
IONIZATION POTENTIAL $V_{ion}$ (volts)
$v_{crit} = \left(\frac{2eV_{ion}}{m_a}\right)^{1/2}$
$10^5$cm/sec
(K)CaMnNiFe
NaAl
MgSi
PS (Cl) Ar
III
[Li] (B) C O (F)
[Be] N Ne
II
$He^4$
H
I
$v_{crit}$ of D-cloud
$v_{crit}$ of C-cloud
$v_{crit}$ of A-cloud
$v_{crit}$ of B-cloud
Fe
Ca
Al
Si
Mg
S
O
C
N
Ne
He
H
$\log \Gamma = \log \frac{eV_{ion}}{\kappa m_a}$
g/cm

Figure 1

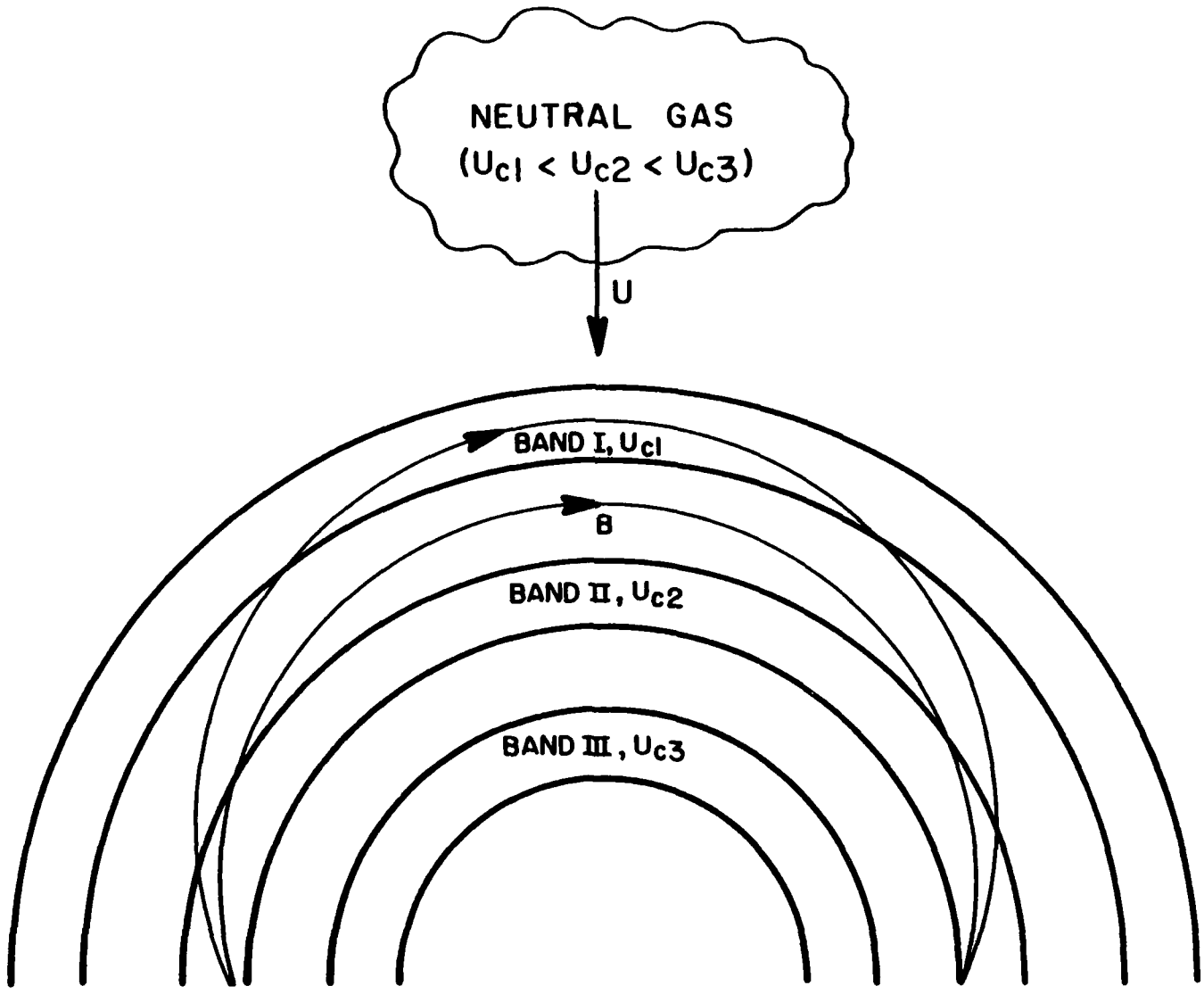


Figure 2

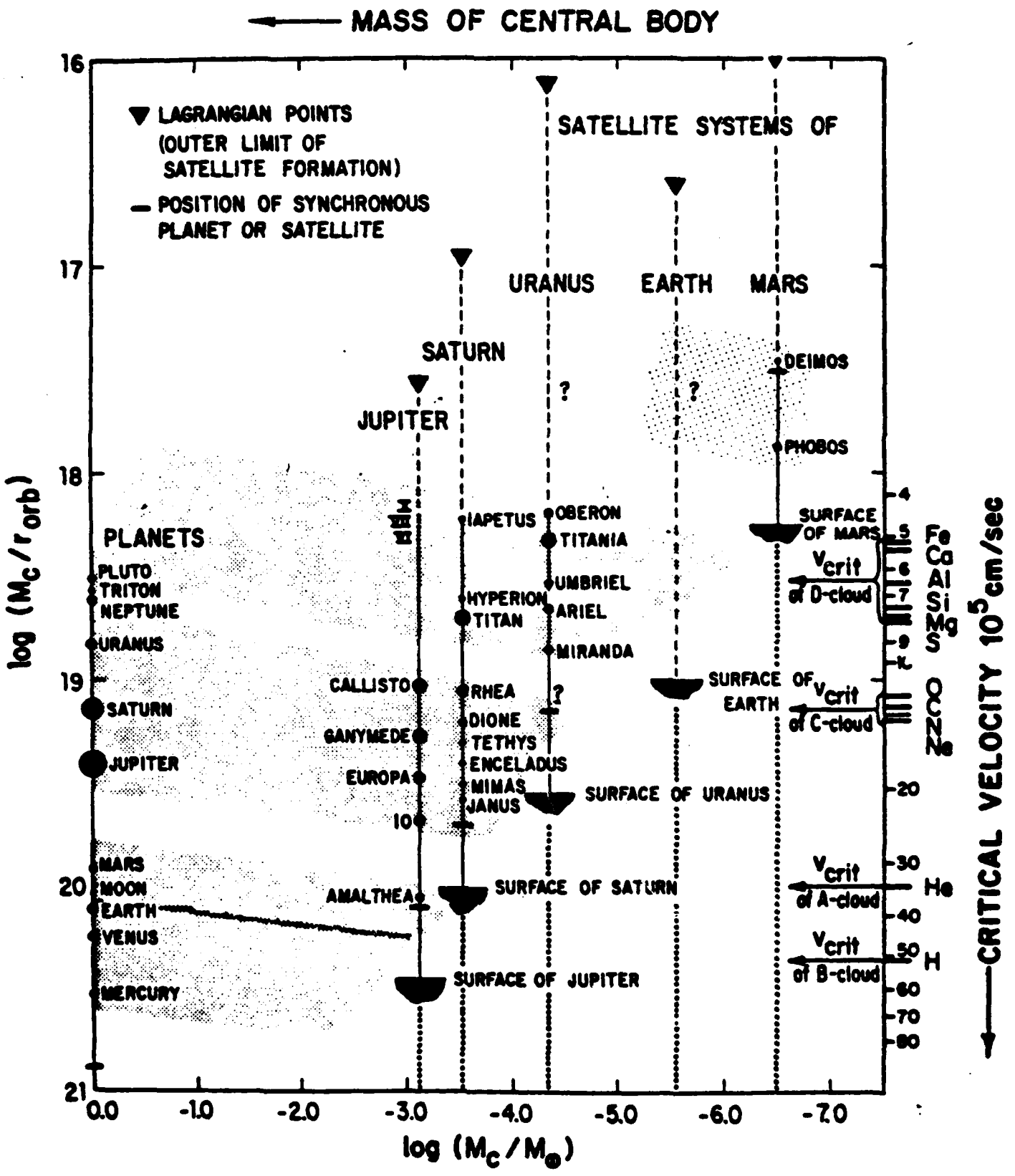
MASS OF CENTRAL BODY
LAGRANGIAN POINTS (OUTER LIMIT OF SATELLITE FORMATION)
POSITION OF SYNCHRONOUS PLANET OR SATELLITE
SATELLITE SYSTEMS OF
JUPITER
SATURN
URANUS
EARTH
MARS
PLANETS
PLUTO
TRITON
NEPTUNE
URANUS
SATURN
JUPITER
MARS
MOON
EARTH
VENUS
MERCURY
CALLISTO
GANYMEDE
EUROPA
AMALTHEA
IAPETUS
HYPERION
TITAN
RHEA
DIONE
TETHYS
ENCELADUS
MIMAS
JANUS
OBERON
TITANIA
UMBRIEL
ARIEL
MIRANDA
DEIMOS
PHOBOS
SURFACE OF JUPITER
SURFACE OF SATURN
SURFACE OF URANUS
SURFACE OF EARTH
SURFACE OF MARS
Vcrit of D-cloud
Vcrit of C-cloud
Vcrit of A-cloud
Vcrit of B-cloud
Fe Ca Al Si Mg S O C Ne
He
H
log (Mc/rorb)
log (Mc/M⊙)
CRITICAL VELOCITY 10^5 cm/sec
16
17
18
19
20
21
0.0
-1.0
-2.0
-3.0
-4.0
-5.0
-6.0
-7.0
4
5
6
7
9
10
20
30
40
50
60
70
80

Figure 3

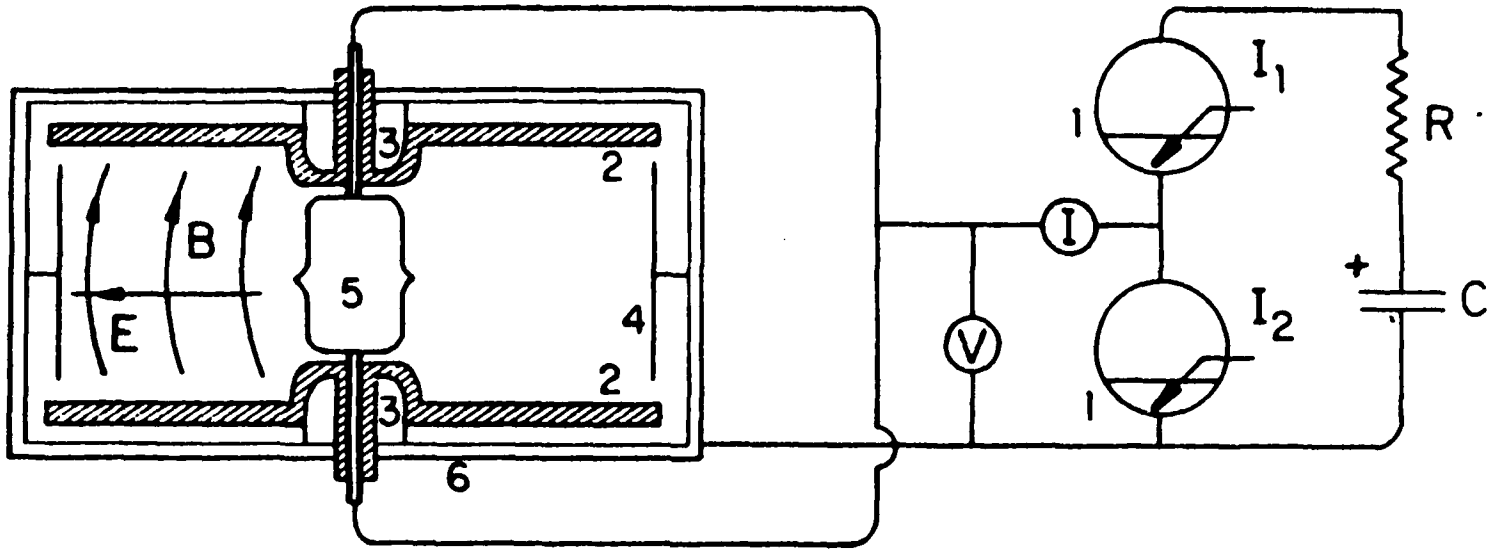


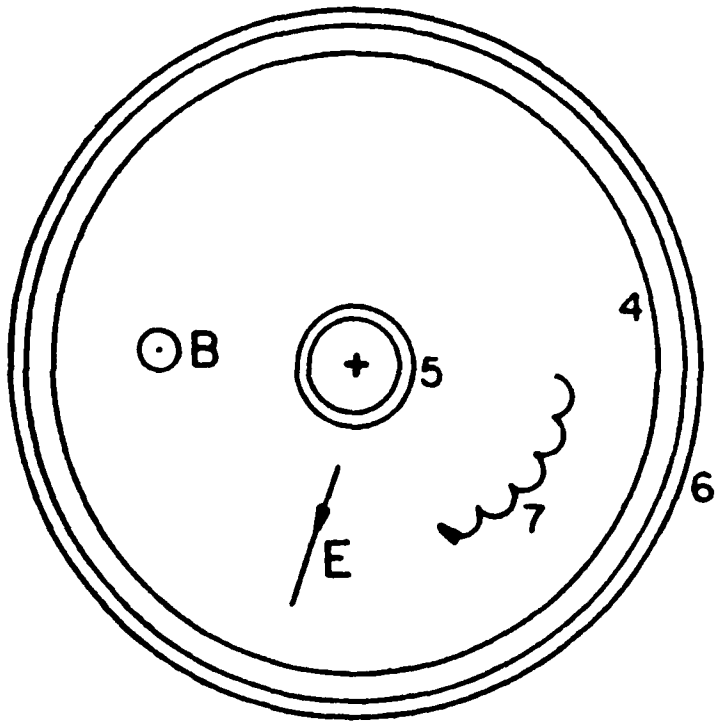


1 Ignitrons
2 Insulators
3 Iron Piece
4 Outer Electrode
5 Inner Electrode
6 Vacuum Tank
7 Typical Particle Orbit

Figure 1

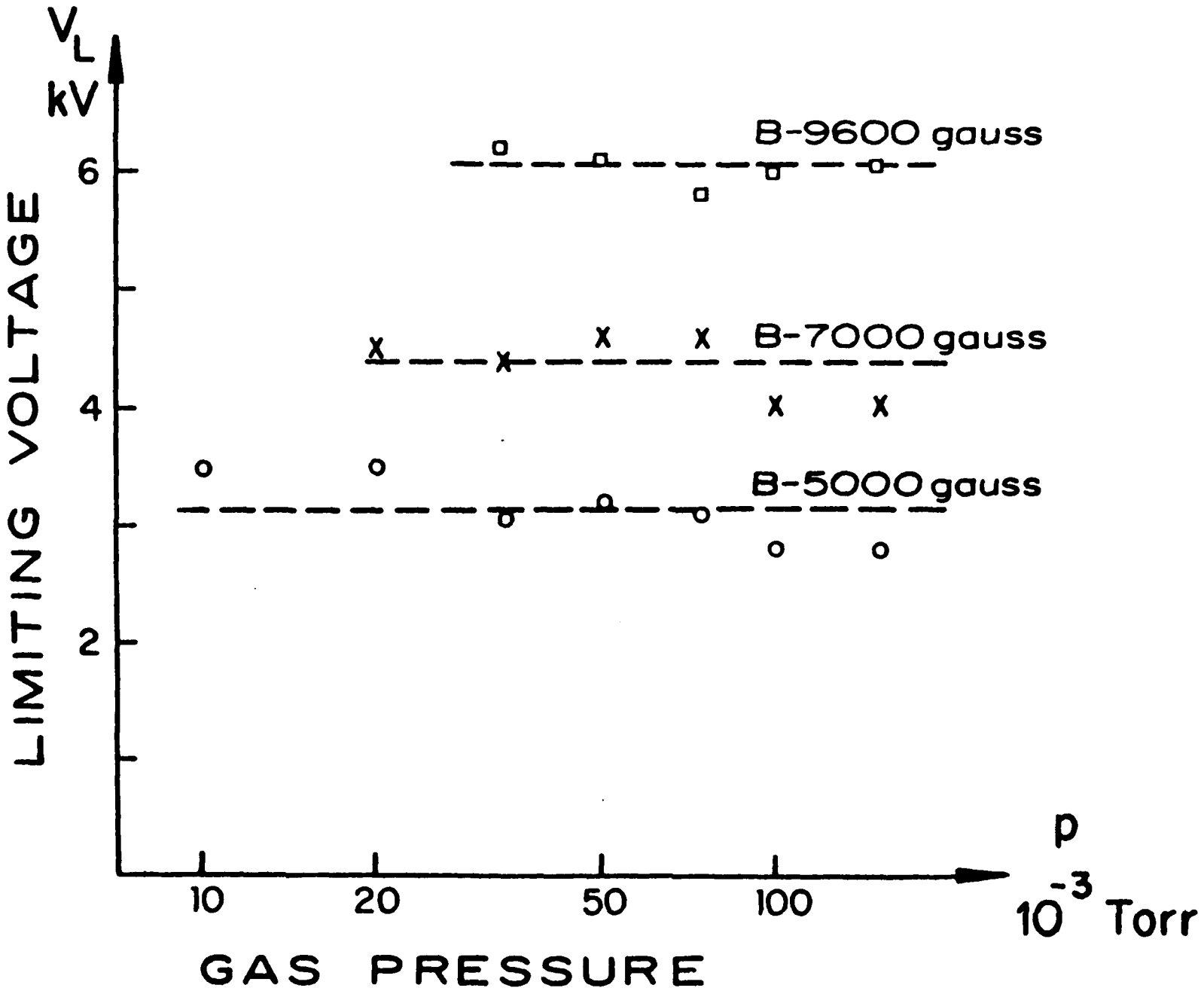
$V_L$
kV
LIMITING VOLTAGE
6
4
2
B-9600 gauss
B-7000 gauss
B-5000 gauss
10
20
50
100
p
$10^{-3}$ Torr
GAS PRESSURE

Figure 5a

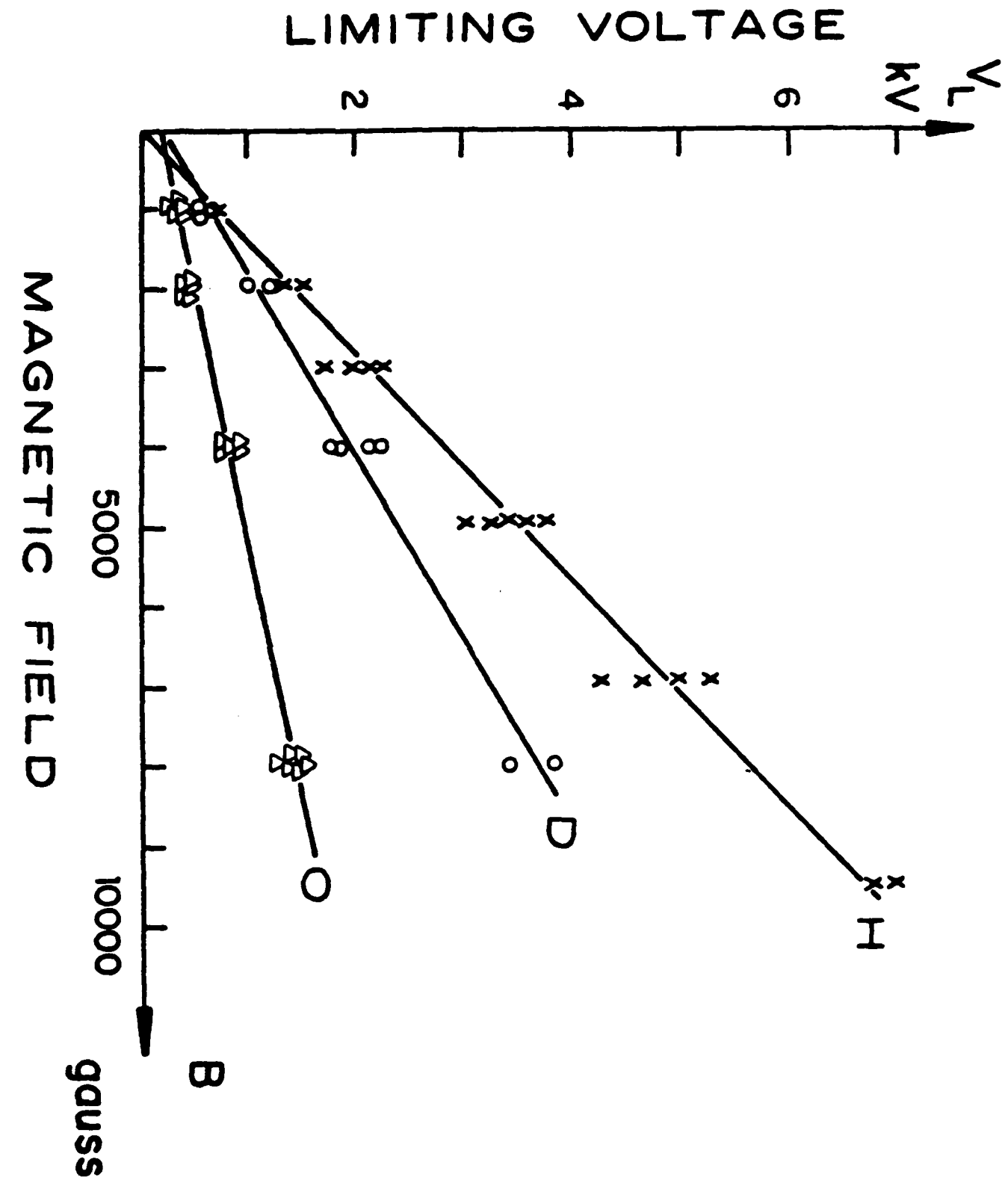
LIMITING VOLTAGE
$V_L$
kV
2
4
6
MAGNETIC FIELD
5000
10000
gauss
B
O
D
H

Figure 5b

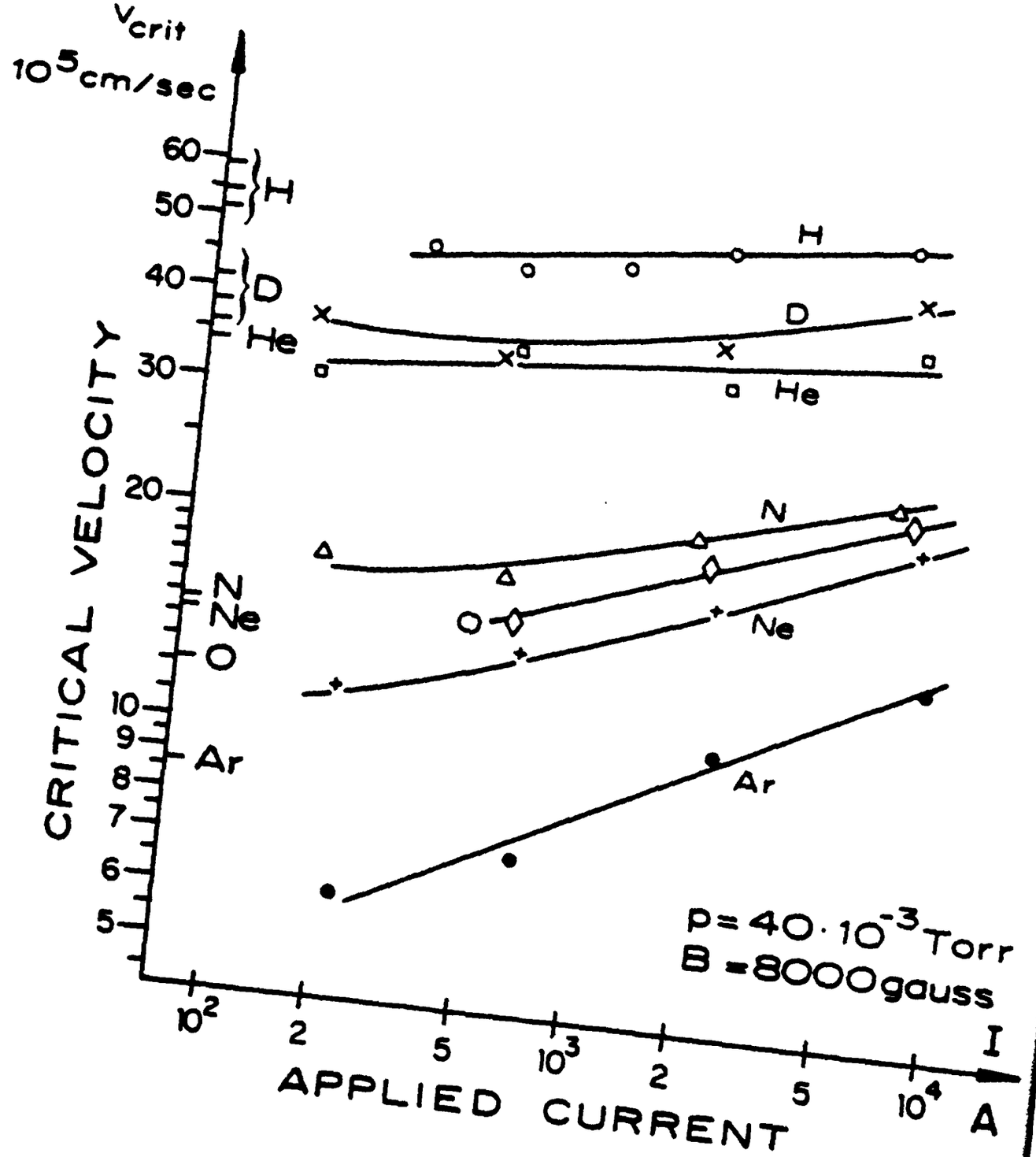
$V_{crit}$
$10^5$cm/sec
CRITICAL VELOCITY
60
50
40
30
20
10
9
8
7
6
5
H
D
He
N
Ne
O
Ar
H
D
He
N
O
Ne
Ar
$p = 40 \cdot 10^{-3}$ Torr
B = 8000 gauss
$10^2$
2
5
$10^3$
2
5
$10^4$
I
A
APPLIED CURRENT

Figure 3c

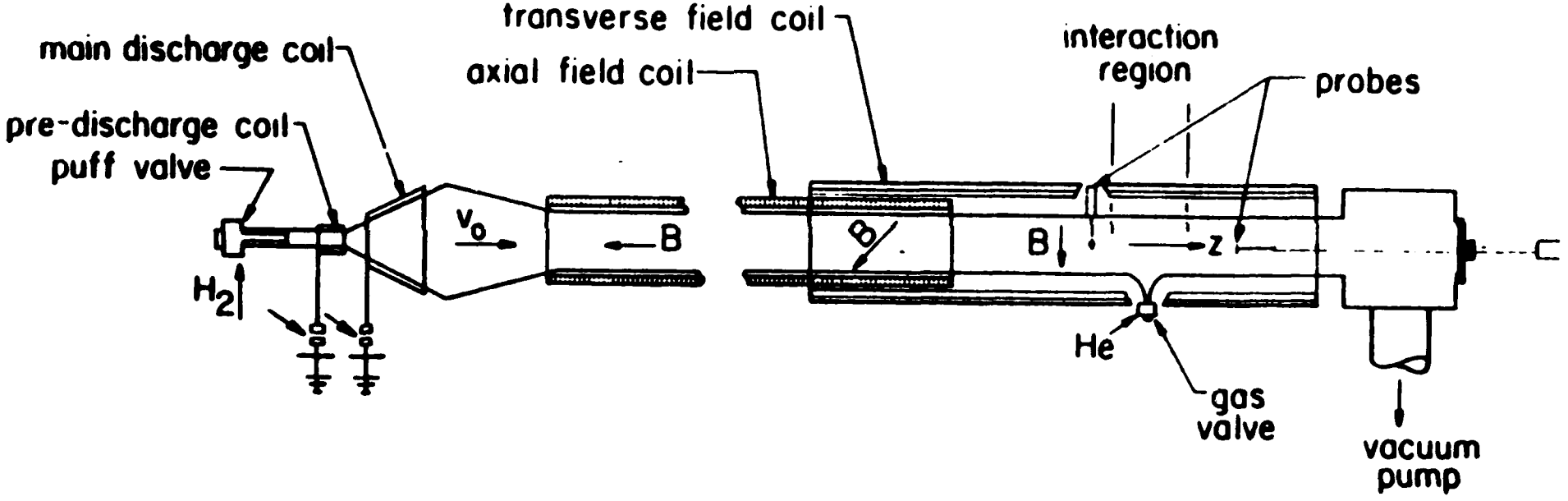
main discharge coil
pre-discharge coil
puff valve
$H_2$
$V_0$
B
transverse field coil
axial field coil
B
B
z
interaction region
probes
He
gas valve
vacuum pump

Figure 6a

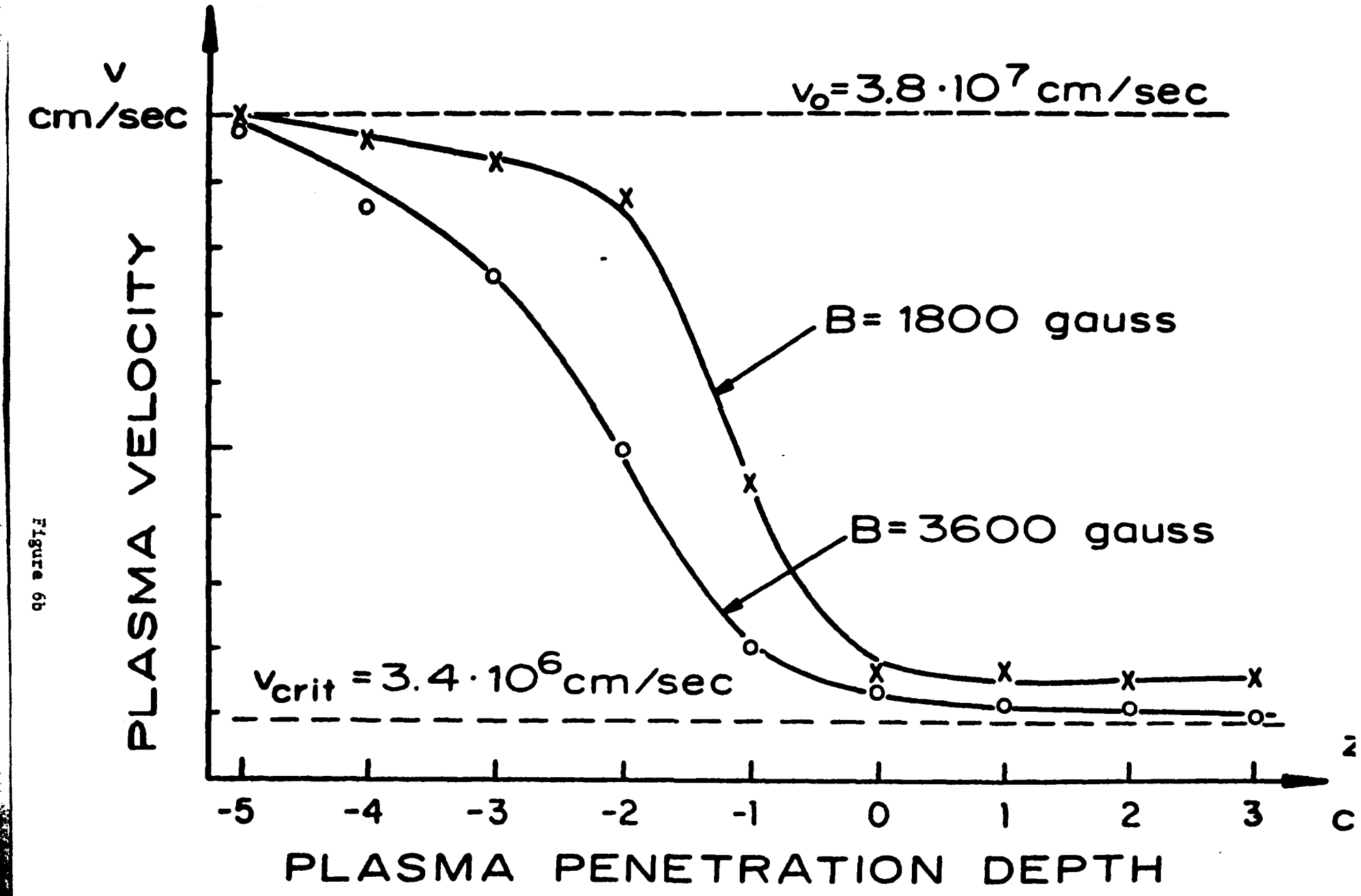
v
cm/sec
$v_o = 3.8 \cdot 10^7$ cm/sec
B = 1800 gauss
B = 3600 gauss
$v_{crit} = 3.4 \cdot 10^6$ cm/sec
PLASMA VELOCITY
-5
-4
-3
-2
-1
0
1
2
3
z
PLASMA PENETRATION DEPTH

Figure 6g

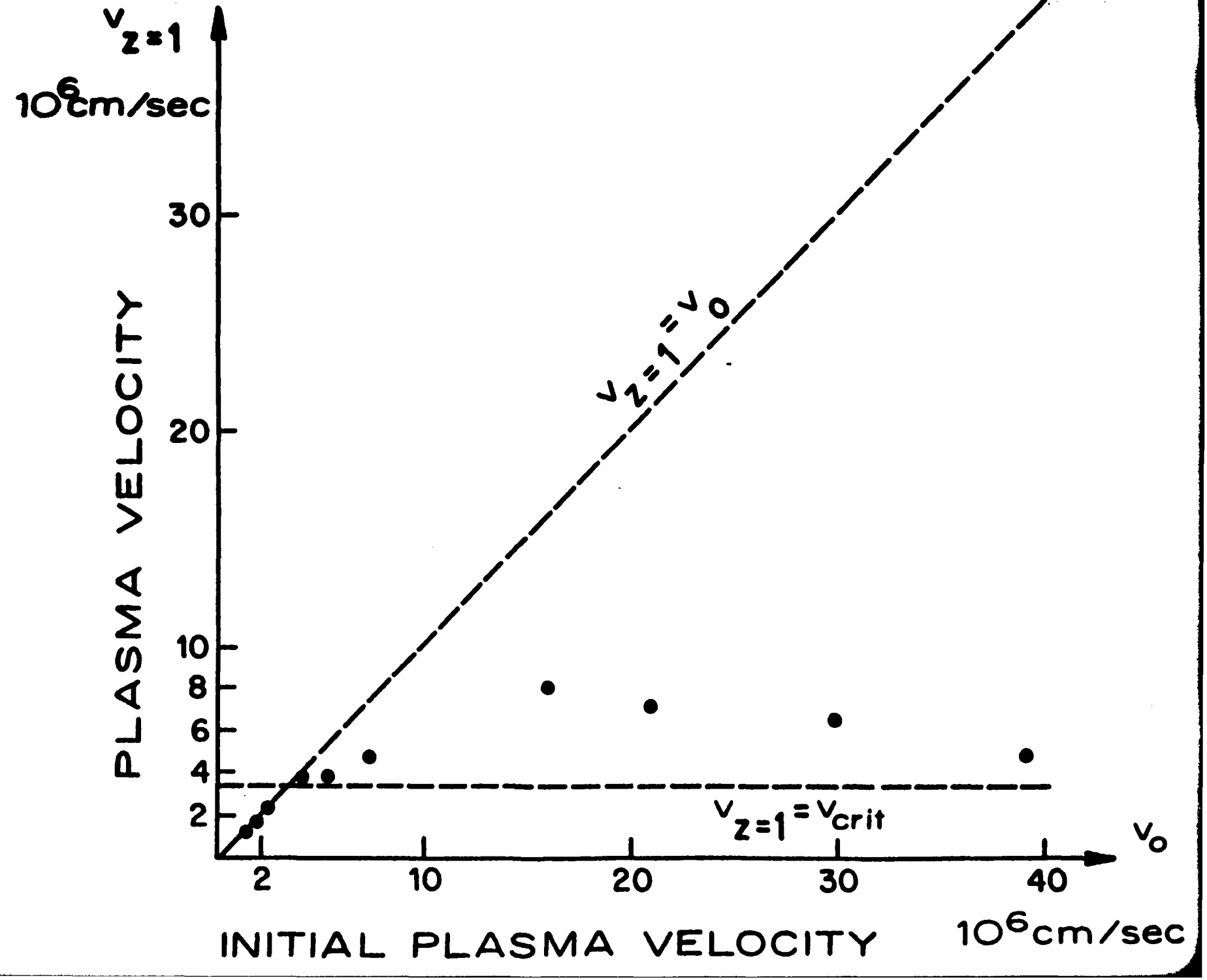
$V_{z=1}$
$10^6$cm/sec
30
20
10
8
6
4
2
PLASMA VELOCITY
$V_{z=1} = V_o$
$V_{z=1} = V_{crit}$
$V_o$
2
10
20
30
40
INITIAL PLASMA VELOCITY
$10^6$cm/sec

Figure 9c

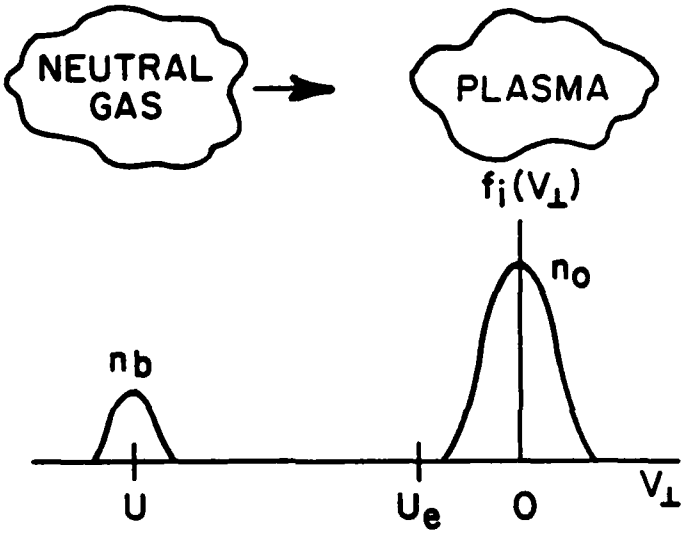


Figure 7

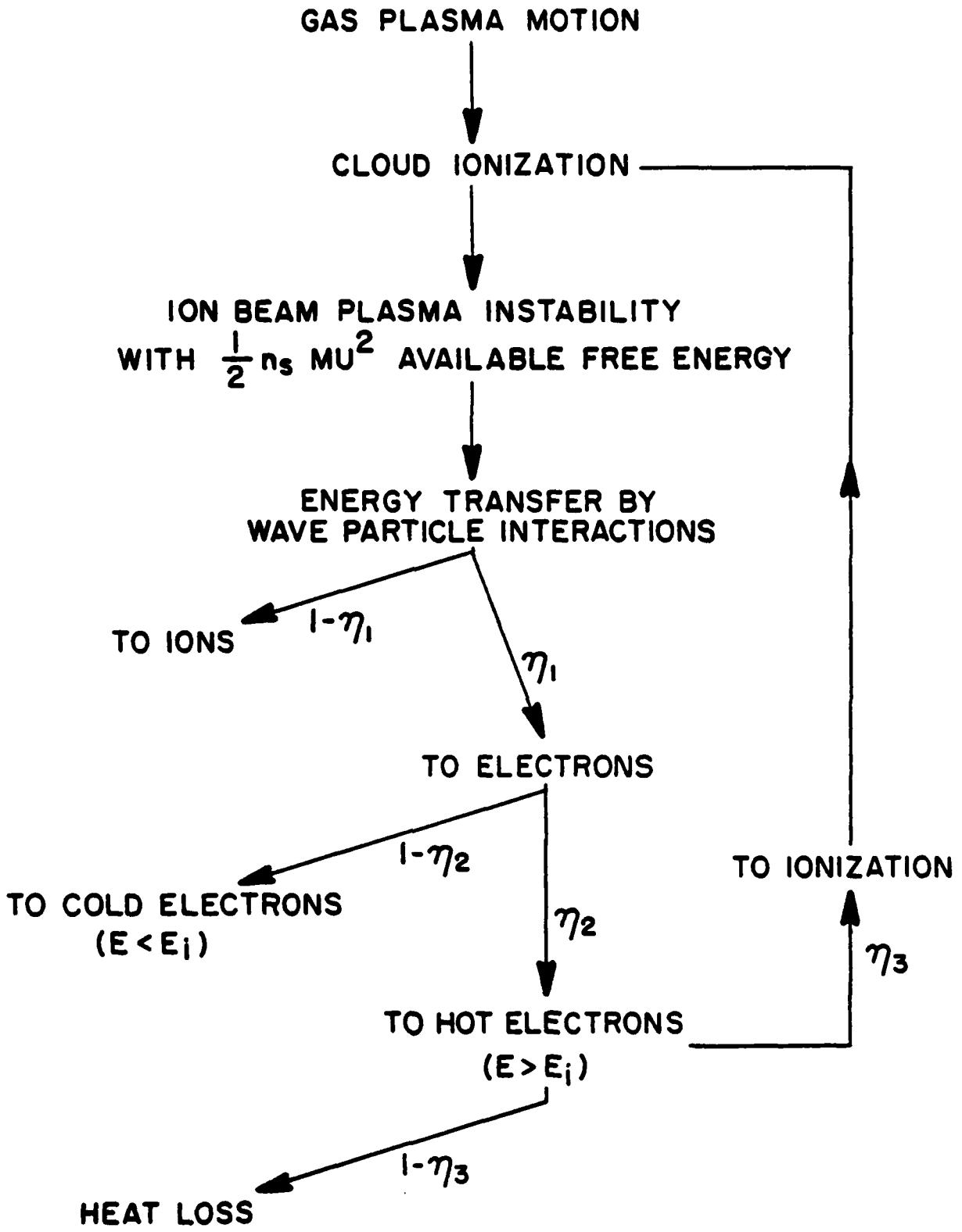
GAS PLASMA MOTION
CLOUD IONIZATION
ION BEAM PLASMA INSTABILITY
WITH $\frac{1}{2} n_s MU^2$ AVAILABLE FREE ENERGY
ENERGY TRANSFER BY
WAVE PARTICLE INTERACTIONS
TO IONS
$1-\eta_1$
$\eta_1$
TO ELECTRONS
$1-\eta_2$
TO COLD ELECTRONS
$(E < E_i)$
$\eta_2$
TO IONIZATION
$\eta_3$
TO HOT ELECTRONS
$(E > E_i)$
$1-\eta_3$
HEAT LOSS

Figure 3

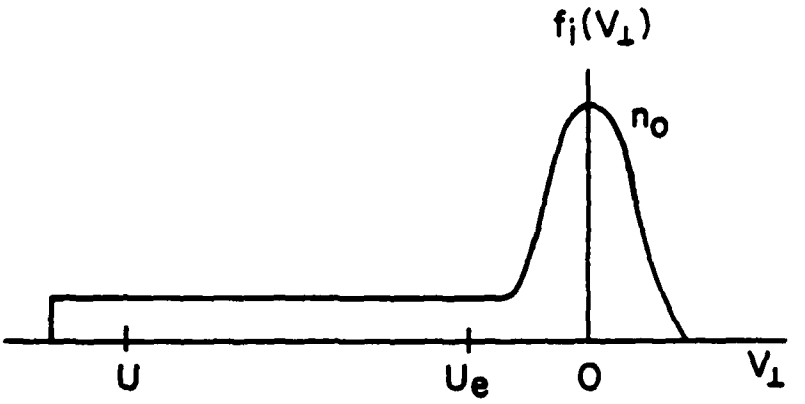


(a)

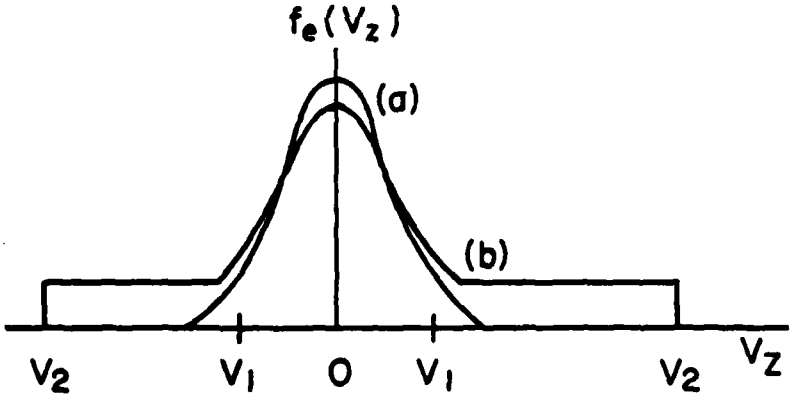


(b)

Figure 9

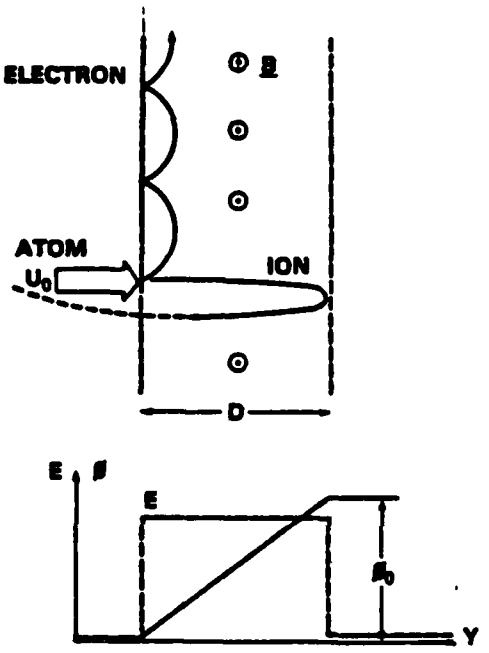
ELECTRON
B
ATOM
$U_0$
ION
D
E
B
E
$B_0$
Y

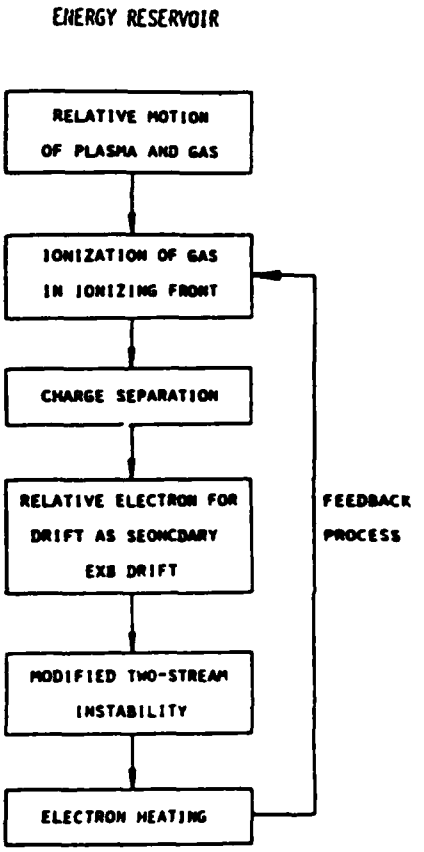
ENERGY RESERVOIR
RELATIVE MOTION OF PLASMA AND GAS
IONIZATION OF GAS IN IONIZING FRONT
CHARGE SEPARATION
RELATIVE ELECTRON FOR DRIFT AS SEONCDARY EXB DRIFT
MODIFIED TWO-STREAM INSTABILITY
ELECTRON HEATING
FEEDBACK PROCESS

Figure 10

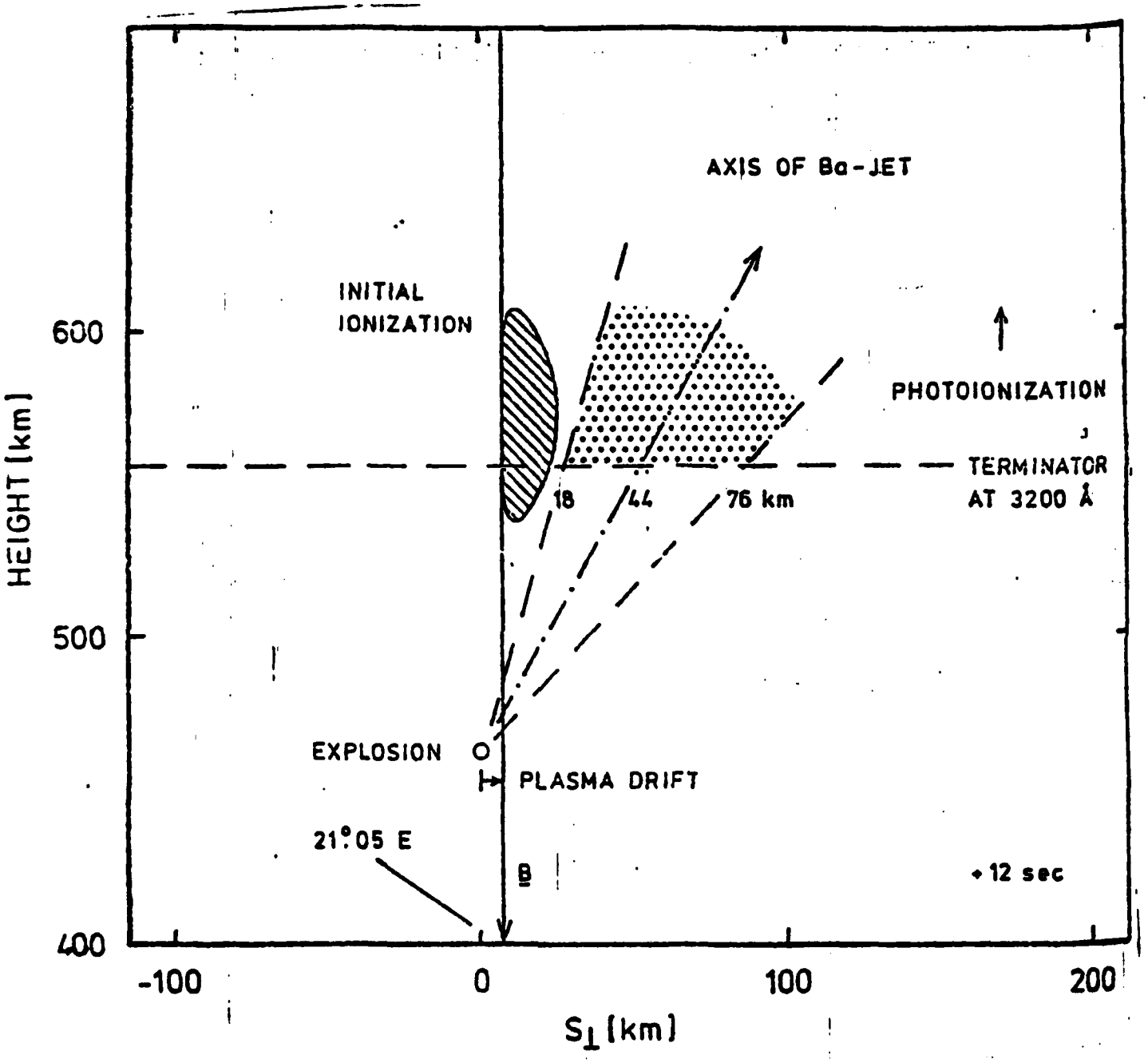
AXIS OF Ba-JET
INITIAL
IONIZATION
PHOTOIONIZATION
TERMINATOR
AT 3200 Å
18
44
76 km
EXPLOSION
O
PLASMA DRIFT
21°05 E
B
+12 sec
HEIGHT [km]
600
500
400
-100
0
100
200
$S_\perp$ [km]

Figure 11

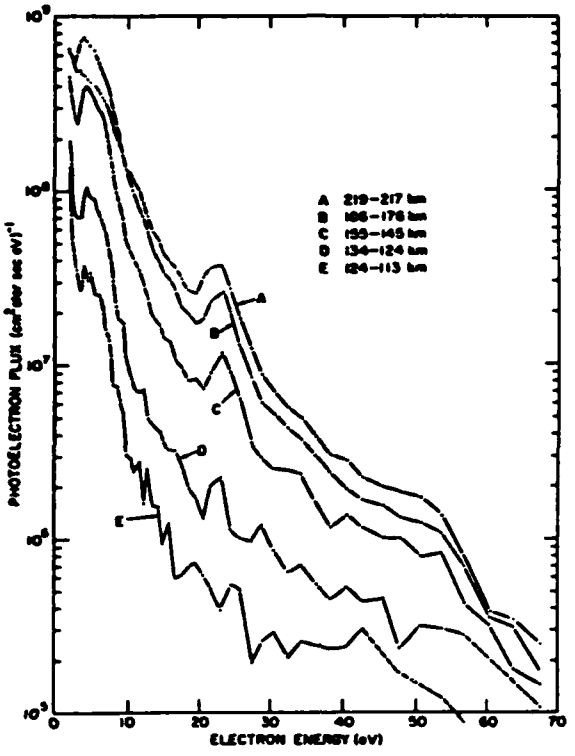
A 219–217 km
B 186–176 km
C 159–145 km
D 134–124 km
E 124–113 km
A
B
C
D
E
PHOTOELECTRON FLUX
ELECTRON ENERGY (eV)
0
10
20
30
40
50
60
70

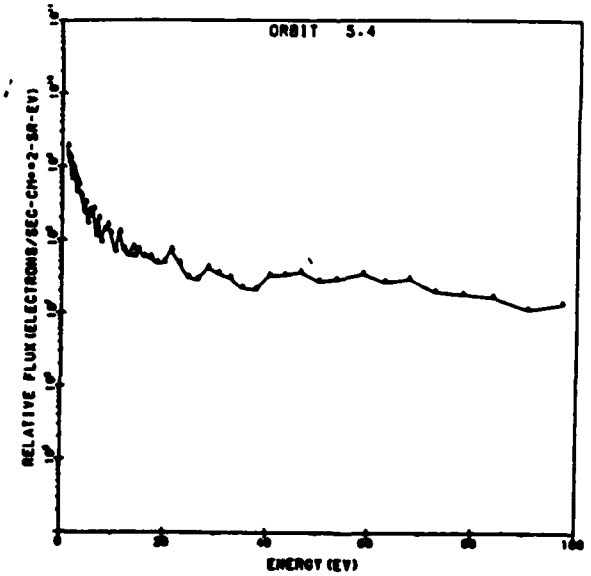
ORBIT 5.4
RELATIVE FLUX (ELECTRONS/SEC-CM**2-SR-EV)
ENERGY (EV)

Figure 12

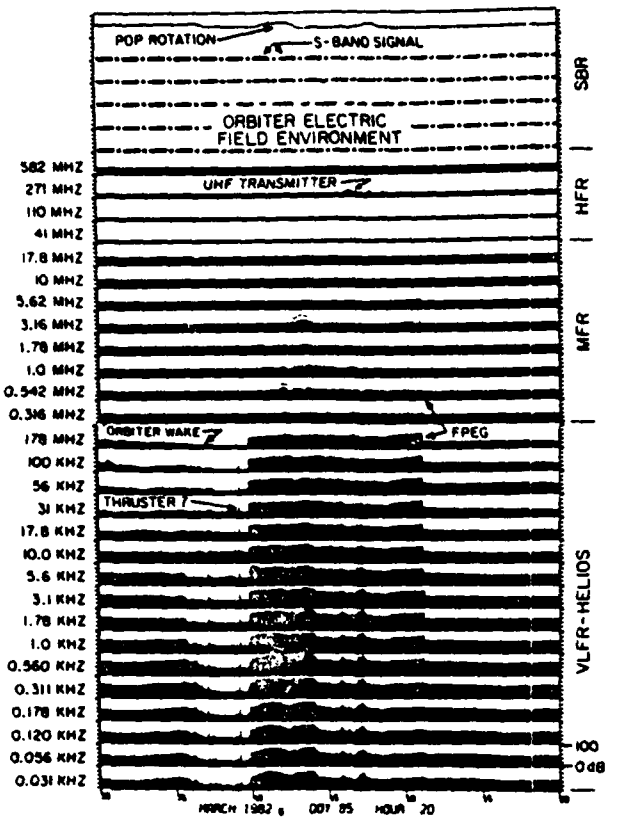


Figure 13

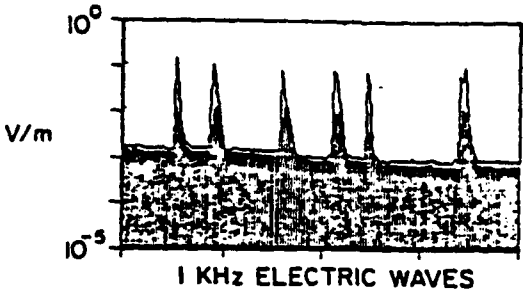


Figure 14